Robust Anticipative Controller Design with Application to A High Dynamic Engine Testbed

Tudor-Bogdan Airimitoaie, Patrick Lanusse, Asma Achnib

Robust Anticipative Controller Design with Application to A High Dynamic Engine Testbed

Tudor-Bogdan Airimitoaie * **Patrick Lanusse** * **Asma Achnib** *

* *Univ. Bordeaux, Bordeaux INP, CNRS, IMS, 33405 Talence, France (e-mail: firstname.lastname@u-bordeaux.fr).*

Abstract: This paper presents a robust controller design method for reference tracking in multi-input multi-output preview systems. In the context of preview systems, it is supposed that future values of the reference signal are available a number of time steps ahead. The objective of the controller being to minimize a quadratic error between the reference and the system's output, the optimal solution needs to take into account the known future values of the reference. Furthermore, it is desired to maintain the control signal at an acceptable level. The feedforward preview is obtained by solving a mixed $\mathcal{L}_2/\mathcal{L}_\infty$ optimisation, where the $\mathcal{L}_\infty$ constraint is used to reduce the level of the control. The proposed solution combines a robust feedback controller with a feedforward preview filter. The feedback controller's purpose is to assure robustness of the closed-loop system to model uncertainties and is not detailed here. The focus of this paper is on the design of the feedforward preview filter taking into account that a feedback controller is present. The proposed solution is validated in simulation on a high dynamic engine testbed.

Keywords: robust control, discrete-time systems, generalized predictive control, feedforward anticipative filter, preview systems.

1. INTRODUCTION

In a number of automatic control applications (known also as preview systems), future values of the reference signal are available in advance. Examples can be found in aeronautical systems (trajectory tracking of unmaned aerial vehicles in Park et al. (2004)), autonomous vehicles (explicit path tracking in Shin et al. (1992)) or mobile robots Freitas et al. (2013). In other applications, disturbance signals can also be known beforehand, such as in water level control (for irrigation and drainage ducts in Schuurmans et al. (1999); Li (2014)). Therefore, it is of interest to propose appropriate control algorithms that take into account this information.

The present paper is focused on the development of discrete-time robust control methods for preview systems. Throughout this paper, it is considered that future values of the reference signal are known a number of time steps ahead. The objective of *preview* is that of designing control algorithms capable of minimizing a quadratic criterion on the error between the plant output and the known future reference. As such, the controller anticipates the future actions that need to be taken with respect to changes of the reference signal and the plant output reacts to these changes before they occur.

The concept of anticipative control (known also as preview control) was proposed initially in Sheridan (1966) and further developed in Tomizuka (1975). A complete review of anticipative control is presented in Liao and Li (2016).

Nevertheless, only a few number of research articles have attempted to deal with the problem of robust anticipative control. In Makarov et al. (2016) an anticipative control problem is considered in the context of motion control of robots. The proposed solution is based on the $\mathcal{H}_\infty$ design methodology. Weighting norms are used to assure robustness of the feedback control law.

A free-weighting matrices technique is used with Lyapunov stability theory to derive robust anticipative controllers in Liao and Li (2016); Li et al. (2017). Both reference anticipative tracking and disturbance rejection are treated; however, an initial design step involves a quadratic criterion which depends on weighting matrices that can be chosen arbitrarily. The proposed method is dependant on the choice of these weighting matrices, which makes it difficult to interpret the obtained results.

The contribution of this paper is to extend the results presented in Achnib et al. (2018a,b) to multi-input multi-output (MIMO) systems and to present a complete theoretical development of the proposed approach. As in Achnib et al. (2018a,b), the robustness considerations take into account both parametric uncertainties and control effort limitations.

A two degrees of freedom feedforward-feedback control schema represents the basis for the proposed controller. A feedforward filter with anticipative behaviour is introduced to take into account future values of the reference signal. It is supposed that the time window of known future reference values is known. The preview window's length of the anticipative feedforward filter can be adjusted accordingly. The feedforward part is obtained by solving a frequency domain optimisation problem with mixed $\mathcal{L}_2$ performance and $\mathcal{L}_\infty$ constraints for robustness. The interesting aspect of the proposed approach is that the

anticipative feedforward action can be added on top of any robust feedback controller.

Simulation results on a 2-inputs 2-outputs high dynamic engine testbed from Lanusse et al. (2016) validate the proposed approach. Testbeds are used in the automobile industry to tune and assess automotive engines. As more High Dynamic (HD) scenarios need to be simulated, the testbeds require MIMO and robust control systems. Furthermore, to improve the accuracy of the results, it is desired to follow the test scenarios as closely as possible. Since the configuration of each scenario is known in advance, it is possible to use this information in a preview controller in order to minimize the tracking error.

The paper is organised as follows. The problem formulation that is addressed in the present paper is described in Section 2. Section 3 introduces the factorisation of the preview feedforward filter that will be used in this paper. Then the optimisation of the unknown part of the filter is presented in Section 4. A solution to reduce the size of this filter is described in Section 5. Simulation results on the high dynamic engine testbed are given in Section 6. Section 7 concludes this paper.

2. PROBLEM FORMULATION

In this paper we use square discrete-time transfer function matrices that we denote with upper-case letters. Signals are denoted with small-case letters in the time-domain and upper-case letters in the frequency-domain. Z-transform variable z is used in the frequency-domain, while in the time-domain we use the unit advance and delay operators q and q^{-1}. $\mathcal{RH}_\infty^{m\times m}$ denotes the set of proper real-rational transfer matrices analytic in $|z|\geq 1$ with m-inputs and m-outputs. Subscripts of transfer function matrix notation indicate input and output signals, i.e. $H_{yu}(z)\in\mathcal{RH}_\infty^{m\times m}$ denotes the transfer function matrix from $u(t)\in\mathbb{R}^m$ to $y(t)\in\mathbb{R}^m$: $Y(z)=H_{yu}(z)U(z)$. We also use right division of vector values signals to indicate the transfer function matrix, such as $Y(z)/U(z)=H_{yu}(z)$.

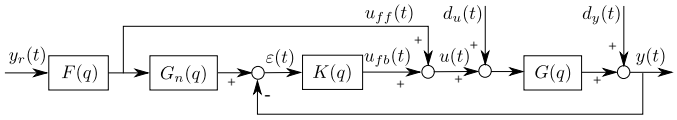

Fig. 1. Feedforward–feedback control schema used for robust anticipative control.

Figure 1 gives a representation of the problem addressed in this paper. The plant, represented by $G(z)\in\mathcal{RH}_\infty^{m\times m}$ belonging to a model-set $\mathcal{M}_G$, is uncertain (or with slowly time-varying parameters) with delays on inputs and/or outputs. The sampling time is T_s and the sampling frequency is f_s.

$K(z)$ denotes the robust feedback controller designed to assure the stability of the feedback loop in the presence of parametric uncertainties and disturbances $d_u(t)\in\mathbb{R}^m$ and $d_y(t)\in\mathbb{R}^m$.

$G_n(z)$ is the nominal plant model chosen from $\mathcal{M}_G$ such that $G_n(z)\in\mathcal{RH}_\infty^{m\times m}$ has only input delays. If the true plant $G(z)=G_n(z)$ and in the absence of disturbances $d_u(t)$ and $d_y(t)$, it can be seen from Fig. 1 that $\varepsilon(t)=0$ and $u_{fb}(t)=0$.

$F(z)$ is the preview feedforward filter that needs to be designed such that the output $y(t)\in\mathbb{R}^m$ of the plant $G(z)$ follows the reference $y_r(t)$ and minimises the ∞-norm of the error

$$\varepsilon_y(t)=y_r(t)-y(t). \tag{1}$$

It is assumed that at any time $a+d$ samples of the reference signal $y_r(t)\in\mathbb{R}^m$ (see also Fig. 1) are known beforehand, where d is the maximum input delay in $G_n(z)$; however, no other assumption is made about the dynamics that generate $y_r(t)$.

The term "preview" is used to indicate that the filter has terms depending on future values of its input. The interpretation of "preview" is better understood in the time-domain, where $F(q)$ has terms in q^{-1} and also in q which depend on future values of this filter's input. This is possible in applications for which future values of the reference or of the disturbances are known beforehand (see discussion in the introduction section).

For robustness, the variability of the true plant model and the limits of the control actuator have to be taken into account in the design of $F(z)$. From the schema in Fig. 1, it can be seen also that the control $u(t)$ is given by the sum of the feedback and feedforward control actions: $u(t)=u_{fb}(t)+u_{ff}(t)$. Thus, the design of $F(z)$ has to take into account also the effects of the feedback loop.

3. FACTORISATION OF THE FEEDFORWARD PREVIEW FILTER

In this section, we introduce a factorisation of $F(z)$ that is useful in the development of the algorithm. We begin by recalling the inner-outer factorisation.

Lemma 1. (Inner-Outer factorisation Vidyasagar (1987)). Let $G(z)\in\mathcal{RH}_\infty^{p\times m}$ have full rank for all $z=e^{j\omega}$. Then $G(z)$ has inner-outer factorisation $G(z)=G_i(z)G_o(z)$, where $G_i(z)\in\mathcal{RH}_\infty^{p\times n}$, $n=\min(p,m)$, is said to be inner if $G_i^T(z^{-1})G_i(z)=I$ and $G_o(z)\in\mathcal{RH}_\infty^{n\times m}$ is outer if it has a right inverse $G_o^{-1}(z)$ which is analytic outside the unit circle. If $p\geq m$, then $G_o(z)$ is square, whereas if $p\leq m$ then $G_i(z)$ is square.

The proof is given in Vidyasagar (1987). Using this lemma, the nominal model $G_n(z)$ with input delays has an inner-outer factorisation

$$G_n(z)=G_i(z)G_o(z)G_d(z), \tag{2}$$

where $G_i(z)$ is the inner factor, $G_o(z)$ is the outer factor and $G_d(z)$ is a $m\times m$ diagonal matrix regrouping the input delay terms.

This suggests the following factorisation of the preview feedforward filter $F(z)$

$$F(z)=F_o(z)T_F(z),\ \text{with}\ F_o(z)=G_d(z^{-1})G_o^{-1}(z). \tag{3}$$

In the previous equation, $G_d(z^{-1})$ is a preview filter depending on future values of its input.

Using the factorisations of $G_n(z)$ and $F(z)$, the schema in Fig. 1 can be simplified as in Fig. 2.

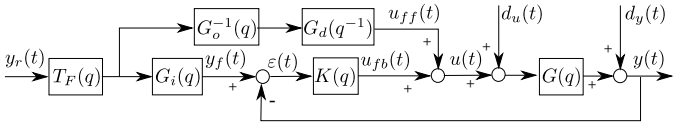

Fig. 2. Feedforward–feedback control schema using factorisation of nominal model and preview feedforward filter.

In (3), $T_F(z)$ is a square diagonal preview filter. Each diagonal term of $T_F(z)$ can be written:

$$T_F(z)(k)=t_{F_{k,-s}}z^{-s}+\ldots+t_{F_{k,-1}}z^{-1}+t_{F_{k,0}} +t_{F_{k,1}}z+\ldots+t_{F_{k,a}}z^{a}, \tag{4}$$

where k indicates the diagonal element ($1 \leq k \leq p$). In the previous equation, s and a give, respectively, the size of the storage and the anticipation horizon of filter $T_F(z)$. The rest of this paper is focused on the design of the preview filter $T_F(z)$ in order to minimize the ∞-norm of the error $\varepsilon_y(t)$ under input $u_{FF}(t)$ constraints and uncertainties of the real plant model $G(z)$.

4. DESIGN OF THE PREVIEW FEEDFORWARD FILTER

This section describes the method used to find the parameters of the preview filter $T_F(z)$. Let denote

$$\theta_k = [t_{F_{k,-s}}, \ldots, t_{F_{k,-1}}, t_{F_{k,0}}, t_{F_{k,1}}, \ldots, t_{F_{k,a}}]^T \tag{5}$$

the adjustable parameters of the diagonal element in (4) and

$$\theta = [\theta_1^T, \ldots, \theta_p^T]^T \tag{6}$$

the vector of all adjustable parameters.

Two closed-loop transfer function matrices in Fig. 2 are of interest. Let us define, in the frequency-domain, the transfer matrix from reference to control input as

$$H_{uy_r}(z) = \\ = (I_m + K(z)G(z))^{-1} \left(G_i(z^{-1})G_o^{-1}(z) + K(z)\right) T_F(z), \tag{7}$$

and the transfer matrix from reference to system output as

$$H_{yy_r}(z) = G(z)H_{uy_r}(z), \tag{8}$$

where I_m is the identity matrix of size m.

Using (1) and (8), the following objective function is defined

$$J_F(\theta) = \sup_t \left|\varepsilon_y(t)\right| \tag{9}$$

$$= \sup_t \left|\left(I_p - H_{yy_r}(q)\right) y_r(t)\right|, \ \forall G(q) \in \mathcal{M}_G. \tag{10}$$

For finite energy reference signals $y_r(t)$, a least upper bound of the previous objective function can be obtained by using the 2-norm [1] (see Doyle et al. (1990)):

$$J_F(\theta) \leq \left\|I_p - H_{yy_r}(e^{j\omega T_s})\right\|_2 \|y_r(t)\|_2. \tag{11}$$

As stated in section 2, the dynamics that generate $y_r(t)$ are unknown, as such the previous objective should be satisfied for any $y_r(t)$, thus only the first term in the right-hand side of the inequality (11) can be optimised. The following minimisation problem is proposed for the unknown parameters θ:

$$\hat{\theta} = \arg\min_{\theta} \ \left\|I_p - H_{yy_r}(e^{j\omega T_s})\right\|_2, \ \forall G(z) \in \mathcal{M}_G. \tag{12}$$

Proposition 2. For diagonal preview filter $T_F(z)$, the minimisation problem given in (12) can be decomposed in p independent minimisations, one for each diagonal element of $T_F(z)$ as in

$$\hat{\theta}_k = \arg\min_{\theta_k} \ \left\|I_p(:,k) - H_{yy_r}(e^{j\omega T_s})(:,k)\right\|_2, \tag{13}$$

where the notation $(:,k)$ is used to indicate the k-th column of the matrix.

Proof. Introducing the p-inputs and p-outputs transfer matrix

$$H_{yy_f}(z) = G(z)\left(I_m + K(z)G(z)\right)^{-1}\left(G_i(z^{-1})G_o^{-1}(z) + K(z)\right),$$

in (7), one obtains

$$H_{yy_r}(z) = H_{yy_f}(z)T_F(z), \tag{14}$$

where

$$T_F(z) = \mathrm{diag}(T_F(z)(i)) = \begin{bmatrix} T_F(z)(1) & & \\ & \ddots & \\ & & T_F(z)(p) \end{bmatrix}. \tag{15}$$

After multiplication on the right-hand side of (14), one obtains

$$H_{yy_r}(z) = \Big[H_{yy_f}(z)(:,1)T_F(z)(1), \ldots, \\ H_{yy_f}(z)(:,p)T_F(z)(p)\Big]. \tag{16}$$

It is straightforward to see that the $\mathcal{L}_2$-norm in (12) simplifies to the sum of the $\mathcal{L}_2$-norms for each column element as in (13) and that the optimum $\hat{\theta}$ is given by the collection of the $\hat{\theta}_k$. ■

Rewritting (4) as $T_F(z)(k) = \phi^T(z)\theta_k$, where θ_k has been defined in (5) and $\phi(z) = [z^{-s}, \ldots, z^{-1}, 1, z, \ldots, z^a]^T$, column k of $H_{yy_r}(z)$ is given by

$$H_{yy_r}(z)(:,k) = H_{yy_f}(z)(:,k)\phi^T(z)\theta_k, \tag{17}$$

which shows that it is linear in the parameters vector θ_k.

Using proposition 2, we define p constrained optimisation problems (one for each θ_k) as

$$\hat{\theta}_k = \arg\min_{\theta_k} \ \left\|I_p(:,k) - H_{yy_r}(e^{j\omega T_s})(:,k)\right\|_2, \tag{18a}$$

$$\text{s.t.} \sum_{l=-s}^{a} \theta_k(l) = 1 \tag{18b}$$

$$\text{and } \left\|W_{uy_r}(e^{j\omega T_s})(i,k)H_{uy_r}(e^{j\omega T_s})(i,k)\right\|_\infty \leq 1, \\ \forall\ 1 \leq i \leq m,\ \omega \in [0, \pi f_s] \text{ and } G(z) \in \mathcal{M}_G. \tag{18c}$$

Two constraints are added to the optimisation problem in (18). The first one, (18b), is introduced to ensure that the steady state gain of $T_F(z)$ has unit value.

In the second one, (18c), the weighting function $W_{uy_r}(z)$ is used to introduce a frequency constraint on the control input $u(t)$. In practice, this is necessary in order to limit the control action at frequencies where the plant model has very low gain.

5. REDUCING THE NUMBER OF PARAMETERS OF THE PREVIEW FEEDFORWARD FILTER

Often in applications, the dynamics of the preview feedforward filter need not be as fast as the other blocs in Fig. 2. It is therefore recommended to choose a slower sampling period for the preview feedforward filter $T_F(z)$ in order to reduce the size of vector θ_i.

Let r denote a sampling time multiplier for the preview feedforward filter. The Z-transform variable and the unit time advance operator for the sampling period $T_{s_r} = r \cdot T_s$ become, respectively, $z_r = z^r$ and $q_r = q^r$. Then $T_F(z_r)$ denotes the anticipative part of the feedforward filter that is sampled at $r \cdot T_s$ seconds with diagonal element:

$$T_F(z_r)(k) = t_{F_{k,-s}} z_r^{-s} + \ldots + t_{F_{k,-1}} z_r^{-1} + t_{F_{k,0}} \\ + t_{F_{k,1}} z_r + \ldots + t_{F_{k,a}} z_r^a, \tag{19}$$

Taking into account the sampling period multiplier r, the sampling frequency for the $T_F(z_r)$ filter in (19) is $f_{s_r} = \frac{f_s}{r}$. As such, z_r becomes in the frequency domain $e^{j\omega_r(rT_s)}$, where $\omega_r \in \left[0, \frac{\pi f_s}{r}\right]$.

[1] For discrete-time operators, the frequency response is obtained by replacing q through $e^{j\omega T_s} = e^{j2\pi f/f_s}$.

To reduce aliasing effects due to $T_F(z)$ which is sampled at a slower frequency, an anti-aliasing filter $H_f(z)$ is introduced at the sampling period T_s as in Fig. 3. The cut-off frequency of $H_f(z)$ is $0.8\frac{f_s}{2r}$. Fig. 3 shows also the separation of sampling times in the control schema.

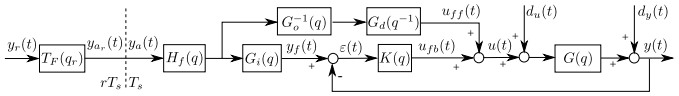

Fig. 3. Feedforward–feedback control schema used for robust anticipative control with sampling rate change and low-pass filter.

The vector valued signal $y_a(t)$ is obtained from $y_{a_r}(t)$ by up-sampling at r times the initial sampling rate and introducing zeros at the new sampling times. Then a filtering through

$$H_{up}(z) = \sum_{n=0}^{r-1} z^{-n}, \tag{20}$$

allows to obtain, in the time-domain, the same result as the initial signal: $y_a((n\cdot r+v)\cdot T_s) = y_{a_r}(n\cdot T_{s_r}),\ \forall\ 0\le v\le r-1$.

The optimisation problem in (18) involves the frequency responses of filters H_{yy_r} and H_{uy_r} which now include both terms sampled at T_s and T_{s_r}.

Let's denote $H_{uy_a}(z)$ the transfer from $Y_a(z)$ to $U(z)$. The following corollary gives the equation defining this transfer.

Lemma 3. The frequency response of the transfer from $Y_r(z_r)$ to $U(z)$, $\forall\omega\in\left[0,\frac{\pi f_s}{r}\right]$, is given by

$$H_{uy_r}(e^{j\omega T_s}) = H_{uy_a}(e^{j\omega T_s})\frac{1}{r}\left(\sum_{n=0}^{r-1} e^{-j\omega T_s n}\right) T_F(e^{j\omega r T_s}). \tag{21}$$

Proof. Using the definition of $H_{uy_a}(z)$, one obtains the frequency response of this transfer function matrix as $H_{uy_a}(e^{j\omega T_s})$, $\forall\omega\in[0,\pi f_s]$. One can restrict its evaluation over the frequencies given by $\omega_r\in\left[0,\frac{\pi f_s}{r}\right]$:

$$U(e^{j\omega_r T_s}) = H_{uy_a}(e^{j\omega_r T_s})Y_a(e^{j\omega_r T_s}),\ \forall\omega_r\in\left[0,\frac{\pi f_s}{r}\right]. \tag{22}$$

At the same time, the frequency response from $Y_r(z_r)$ to $Y_{a_r}(z_r)$ is given by

$$Y_{a_r}(e^{j\omega_r(rT_s)}) = T_F(e^{j\omega_r(rT_s)})Y_r(e^{j\omega_r(rT_s)}), \forall\omega_r\in\left[0,\frac{\pi f_s}{r}\right] \tag{23}$$

Using the Discrete Fourier Transform (DFT) definition for N samples of the vector valued signal $y_{a_r}(t)$:

$$Y_{a_r}(k) = \frac{1}{N}\sum_{n=0}^{N-1} y_{a_r}(n)e^{-j2\pi\frac{kn}{N}},\ \forall\ 0\le k\le N-1. \tag{24}$$

Let's denote by $y_{a_r up}(t)$ the result of the up-sampling of $y_{a_r}(t)$:

$$y_{a_r up}(n\cdot r+v) = \begin{cases} y_{a_r}(n), & \text{if } v=0\\ 0, & \text{otherwise.}\end{cases} \tag{25}$$

One can compute the DFT of rN samples of $y_{a_r up}(t)$:

$$Y_{a_r up}(k) = \frac{1}{rN}\sum_{n=0}^{rN-1} y_{a_r up}(n)e^{-j2\pi\frac{kn}{rN}},\ \forall\ 0\le k\le rN-1 \tag{26}$$

Introducing the change of notation $n = w\cdot r+v$, with $0\le w\le N-1$ and $0\le v\le r-1$, and using (25) for $0\le k\le N-1$:

$$Y_{a_r up}(k) = \frac{1}{rN}\sum_{w=0}^{N-1}\sum_{v=0}^{r-1} y_{a_r up}(w\cdot r+v)e^{-j2\pi\frac{k(w\cdot r+v)}{rN}} \tag{27}$$

$$= \frac{1}{rN}\sum_{w=0}^{N-1} y_{a_r}(w)e^{-j2\pi\frac{kwr}{rN}} \tag{28}$$

$$= \frac{1}{r}Y_{a_r}(k),\ \forall\ 0\le k\le N-1. \tag{29}$$

From (20), (22), (23), and (29), one obtains

$$U(e^{j\omega_r T_s})/Y_r(e^{j\omega_r(rT_s)}) = U(e^{j\omega_r T_s})/Y_a(e^{j\omega T s})\cdot$$
$$Y_a(e^{j\omega T s})/Y_{a_r}(e^{j\omega_r(rT_s)})\cdot Y_{a_r}(e^{j\omega_r(rT_s)})/Y_r(e^{j\omega_r(rT_s)})$$
$$= H_{uy_a}(e^{j\omega_r T_s})\frac{1}{r}\left(\sum_{n=0}^{r-1} e^{-j\omega_r T_s n}\right) T_F(e^{j\omega_r(rT_s)}), \forall\omega_r\in\left[0,\frac{\pi f_s}{r}\right],$$

which proves Lemma 3. ■

Corollary 4. The frequency response of the transfer from $Y_r(z_r)$ to $Y(z)$ for $\omega\in\left[0,\frac{\pi f_s}{r}\right]$ is given by

$$H_{yy_r}(e^{j\omega T_s}) =$$
$$= G(e^{j\omega T_s})H_{uy_a}(e^{j\omega T_s})\frac{1}{r}\left(\sum_{n=0}^{r-1} e^{-j\omega T_s n}\right) T_F(e^{j\omega r T_s}). \tag{30}$$

Using (21) and (30), the optimisation problem (18) can be solved for $\omega\in\left[0,\frac{\pi f_s}{r}\right]$.

6. APPLICATION TO A HIGH DYNAMIC ENGINE TESTBED

In this section, we present simulation results on a high dynamic engine (HDE) testbed obtained using the preview feedforward approach described in this paper. First, section 6.1 describes the testbed used for simulations. Finally, section 6.2 shows results obtained using the preview feedforward filter. The testbed and the feedback controller have been previously presented in Lanusse et al. (2016).

6.1 Description of the High Dynamic Engine Testbed

Dynamic combustion engine testbeds are used for many purposes, such as calibration, driving cycles, control development and research. The simulation system used in this paper is based on the HDE testbed used in Lanusse et al. (2016), which is available at the PRISME laboratory in Orléans, France. It can be used to test combustion, hybrid or electric vehicle engines. A HDE testbed consists of a vehicle engine to be tested and a dynamic mechanical load provided by an electrical machine. Here, the test engine is a Peugeot S.A. EB2, 1.2 liter 3-cylinder Spark Ignition (SI) engine with a maximum power of 60 kW, a maximum torque of 116 Nm and a maximum speed of 4500 rpm. This engine is controlled by a fully open engine control unit (ECU) with $T_s = 5$ ms sampling time. The load is provided by an asynchronous MDA 250 KW machine driven by ABB technology (see also schema in Fig. 4).

The outputs to be controlled are the engine speed and torque (see Fig. 4). The control inputs are the desired current that feeds the electrical machine and the throttle (accelerator pedal) position. Thus, the HDE testbed is a 2-inputs 2-outputs system:

$$\begin{bmatrix} Y_1(z)\\ Y_2(z)\end{bmatrix} = \begin{bmatrix} G_{11}(z) & G_{12}(z)\\ G_{21}(z) & G_{22}(z)\end{bmatrix}\begin{bmatrix} U_1(z)\\ U_2(z)\end{bmatrix} \tag{31}$$

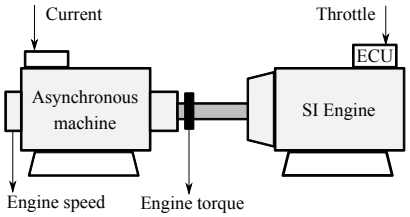

Fig. 4. High dynamic engine testbed schema.

20 operating points have been taken into account for system identification and control. These points have been chosen such that the engine speed varies from 2150 to 3800 rpm (rotations per minute) and the torque from 15% to 75% of the highest torque that the engine can provide for each speed (more details are given in Lanusse et al. (2016)). An operating point at 2590 rpm and 52 Nm has been arbitrarily chosen to define a nominal model. A frequency domain identification of the 21 models has been done and Fig. 5 shows the magnitude and phase plots of all models. One can remark significant variation in both magnitude and phase. The nominal model transfer function matrix is given by (32).

6.2 Simulation results using the proposed anticipative approach

The preview feedforward filter approach is evaluated in simulation using the HDE testbed and CRONE feedback controller developed in Lanusse et al. (2016).

A sampling period multiplier $r = 20$ has been chosen. The anticipation order is $a = 5$ while the storage coefficient of the feedforward filter is $s = 4$. The optimisation has been done using *fmincon* in Matlab. All 20 models plus the nominal model have been used. The $T_F(z_r)$ filter that satisfies the optimisation problem is given in (33).

$$\begin{aligned} T_{F_{11}}(z_r) =& 0.0183z_r^5 + 0.0464z_r^4 + 0.0955z_r^3 + 0.202z_r^2 + \\ & 0.375z_r^1 + 0.0852 + 0.151z_r^{-1} + 0.00637z_r^{-2} + \\ & 0.0495z_r^{-3} - 0.0289z_r^{-4}, \end{aligned} \tag{33a}$$

$$T_{F_{12}}(z_r) = 0, \qquad T_{F_{21}}(z) = 0, \tag{33b}$$

$$\begin{aligned} T_{F_{22}}(z_r) =& 0.178z_r^5 + 0.0997z_r^4 + 0.126z_r^3 + 0.0495z_r^2 + \\ & 0.0899z_r^1 + 0.0135 + 0.0672z_r^{-1} + 0.109z_r^{-2} + \\ & 0.0953z_r^{-3} + 0.172z_r^{-4}. \end{aligned} \tag{33c}$$

Figures 6, 7, 8, and 9 show simulation results using the preview feedforward + robust feedback control presented in this paper. The reference signals $y_r(t)$ are the same as in the previous subsection. The simulations show the variation of control inputs and system outputs around the equilibrium of each linearised model. It can be observed that the two outputs anticipate the changes of the references before they actually occur. Furthermore, the feedforward reduces the chattering in the outputs and input signals with respect to the feedback controller alone.

7. CONCLUSIONS

In this paper, we have presented an algorithm for the design of preview feedforward filters for MIMO systems. The proposed approach considers robustness to plant model uncertainties and control level constraints. Simulation results on a high dynamic engine testbed validate the proposed control. As shown in Lanusse et al. (2016), a judicious choice of a simplified nominal model allows to synthesise a feedback CRONE controller with improved performances for the engine speed control and an improved decoupling from the torque control. The resulting control-system will be assessed using a cycle based on the dynamic part of the non-road transient cycle (NRTC) test.

REFERENCES

Achnib, A., Airimitoaie, T.B., Lanusse, P., Abrashov, S., Aoun, M., and Chetoui, M. (2018a). Discrete-Time Robust Control With an Anticipative Action for Preview Systems. *Journal of Dynamic Systems, Measurement, and Control*, 141(3). doi: 10.1115/1.4041711. 031012.

Achnib, A., Airimitoaie, T.B., Lanusse, P., Guefrachi, A., Aoun, M., and Chetoui, M. (2018b). Anticipative Robust Design Applied to a Water Level Control System. In *2018 17th European Control Conference (ECC)*, 863–869. IEEE, Limassol, Cyprus.

Doyle, J.C., Francis, B.A., and Tannenbaum, A.R. (1990). *Feedback control theory*. Macmillan Publishing Co.

Freitas, G., Lizarralde, F., Hsu, L., and Bergerman, M. (2013). Terrain model-based anticipative control for articulated vehicles with low bandwidth actuators. In *Robotics and Automation (ICRA), 2013 IEEE International Conference on*, 382–389. doi:10.1109/ICRA.2013.6630604.

Lanusse, P., Gruel, D.N., Lamara, A., Lesobre, A., Wang, X., Chamaillard, Y., and Oustaloup, A. (2016). Development of a fractional order based mimo controller for high dynamic engine testbeds. *Control Engineering Practice*, 56, 174 – 189. doi:https://doi.org/10.1016/j.conengprac.2016.06.009.

Li, L., Liao, F., and Deng, J. (2017). H_∞ preview control of a class of uncertain discrete-time systems. *Asian Journal of Control*.

Li, Y. (2014). Offtake feedforward compensation for irrigation channels with distributed control. *IEEE Transactions on Control Systems Technology*, 22(5), 1991–1998. doi: 10.1109/TCST.2013.2294683.

Liao, F. and Li, L. (2016). Robust preview tracking control for a class of uncertain discrete-time systems. *Cogent Engineering*, 3(1), 1243033.

Makarov, M., Grossard, M., Rodríguez-Ayerbe, P., and Dumur, D. (2016). Modeling and preview H_∞ control design for motion control of elastic-joint robots with uncertainties. *IEEE Transactions on Industrial Electronics*, 63(10), 6429–6438.

Park, S., Deyst, J., and How, J. (2004). A new nonlinear guidance logic for trajectory tracking. In *AIAA Guidance, Navigation, and Control Conference and Exhibit*. American Institute of Aeronautics and Astronautics. doi:10.2514/6.2004-4900.

Schuurmans, J., Hof, A., Dijkstra, S., Bosgra, O.H., and Brouwer, R. (1999). Simple water level controller for irrigation and drainage canals. *Journal of Irrigation and Drainage Engineering*, 125(4), 189–195. doi:10.1061/(ASCE)0733-9437(1999)125:4(189).

Sheridan, T.B. (1966). Three models of preview control. *IEEE Transactions on Human Factors in Electronics*, (2), 91–102.

Shin, D.H., Singh, S., and Lee, J.J. (1992). Explicit path tracking by autonomous vehicles. *Robotica*, 10, 539–554. doi:10.1017/S0263574700005865.

Tomizuka, M. (1975). Optimal continuous finite preview problem. *IEEE transactions on automatic control*, 20(3), 362–365.

Vidyasagar, M. (1987). *Control System Synthesis: A Factorization Approach*. The MIT Press, Cambridge, MA, USA, second printing edition.

$$G_{11}(z) = z^{-3}\frac{-0.644 + 1.98z^{-1} - 2.12z^{-2} + 0.669z^{-3} + 0.294z^{-4} - 0.173z^{-5}}{1 - 4.29z^{-1} + 7.56z^{-2} - 6.82z^{-3} + 3.15z^{-4} - 0.591z^{-5}} \tag{32a}$$

$$G_{12}(z) = z^{-15}\frac{0.148 - 0.508z^{-1} + 0.665z^{-2} - 0.383z^{-3} + 0.064z^{-4} + 0.0135z^{-5}}{1 - 4.59z^{-1} + 8.64z^{-2} - 8.35z^{-3} + 4.16z^{-4} - 0.851z^{-5}} \tag{32b}$$

$$G_{21}(z) = z^{-2}\frac{0.0919 + 0.00408z^{-1} - 0.293z^{-2} + 0.223z^{-3} - 0.0255z^{-4} - 0.00105z^{-5}}{1 - 4.01z^{-1} + 6.56z^{-2} - 5.46z^{-3} + 2.27z^{-4} - 0.371z^{-5}} \tag{32c}$$

$$G_{22}(z) = z^{-20}\frac{1.07e-06 + 0.149z^{-1} - 0.524z^{-2} + 0.702z^{-3} - 0.427z^{-4} + 0.0995z^{-5}}{1 - 4.34z^{-1} + 7.74z^{-2} - 7.08z^{-3} + 3.32z^{-4} - 0.635z^{-5}} \tag{32d}$$

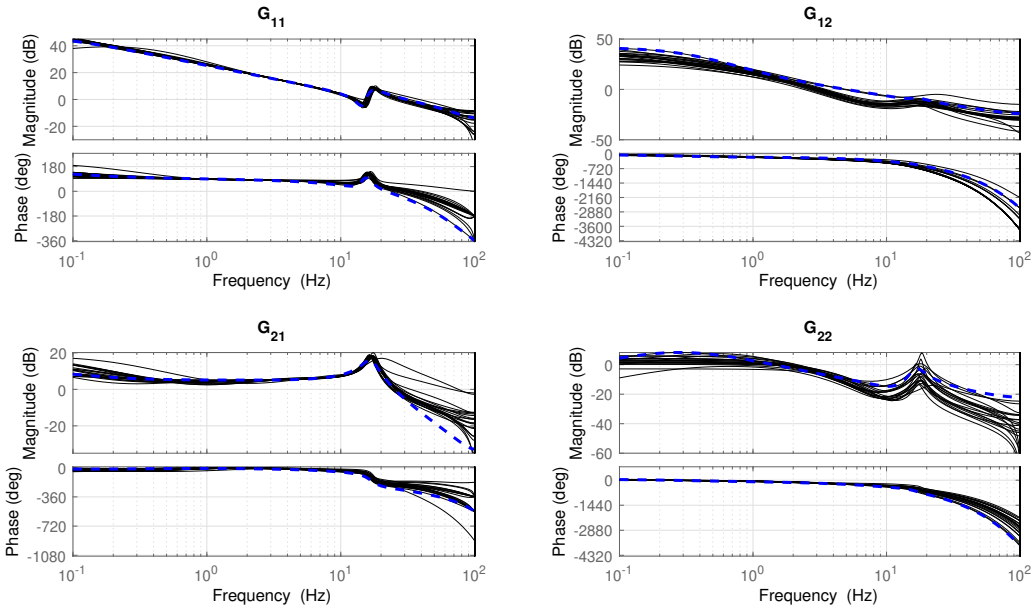

Fig. 5. Bode diagram for 20 operating points (solid black line) and for the nominal model (dashed blue line).

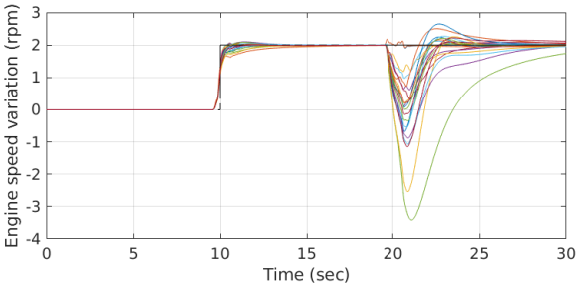

Fig. 6. Engine speed control using feedback and preview feedforward.

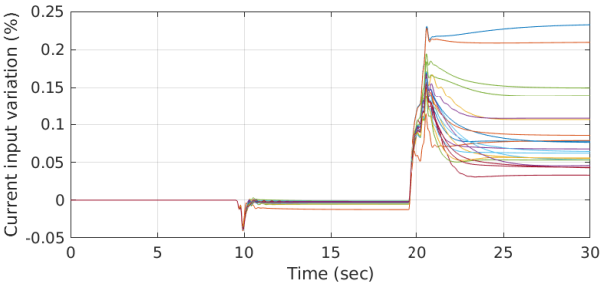

Fig. 8. Current input using feedback and preview feedforward.

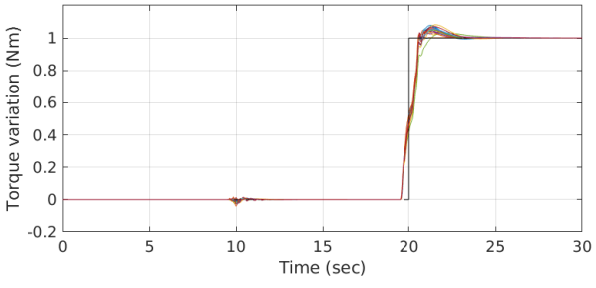

Fig. 7. Engine torque control using feedback and preview feedforward.

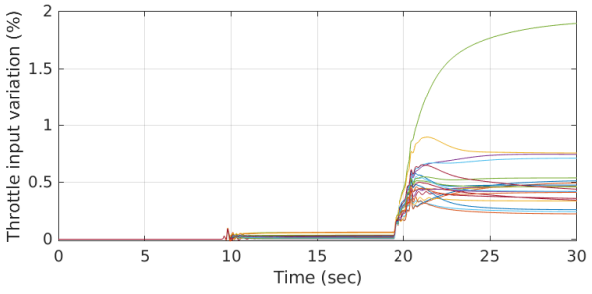

Fig. 9. Throttle input using feedback and preview feedforward.